Shake to the Beat: Exploring the Seismic Signals and Stadium Response of Concerts and Music Fans

Gabrielle Tepp[1], Igor Stubailo[1], Monica Kohler[2], Richard Guy[3], Yousef Bozorgnia[3]

1. Seismological Laboratory, Caltech, Pasadena, CA
2. Department of Mechanical and Civil Engineering, Caltech, Pasadena, CA
3. Department of Civil and Environmental Engineering, UCLA, Los Angeles, CA

Corresponding author: G. Tepp, 1200 E. California Blvd, 252-21, Pasadena, CA, 91125

Declaration of Competing Interests

The authors acknowledge there are no conflicts of interest recorded.

Abstract

Large music festivals and stadium concerts are known to produce unique vibration signals that resemble harmonic tremor, particularly at frequencies around 1-10 Hz. This study investigates the seismic signals of a Taylor Swift concert performed on 5 August 2023 (UTC) as part of a series at SoFi Stadium in Inglewood, CA, with an audience of ~70,000. Signals were recorded on regional seismic network stations located within ~9 km of the stadium, as well as on strong-motion sensors placed near and inside the stadium prior to the concert series. We automatically identified the low-frequency signals from spectrograms using a Hough transform approach and characterized their start times, durations, frequency content, particle motions, radiated energy, and equivalent magnitudes. These characteristics allowed us to associate the signals with individual songs and explore the nature of the seismic source. The signal frequencies matched the song beat rates well, whereas the signal and song durations were less similar. Radiated energy was determined to be a more physically-relevant measure of strength than magnitude given the tremor-like nature of the signals. The structural response of the stadium showed nearly equal shaking intensities in the vertical and horizontal directions at frequencies that match the seismic signals recorded outside the stadium. Additionally, we conducted a brief experiment to further evaluate whether the low-frequency signals could be generated by the speaker system and instruments, audience motions, or something else. All evidence considered, we interpret the signal source as primarily crowd motion in response to the music. Particle motions of the strongest harmonics are consistent with Rayleigh waves influenced by scattered body waves and likely reflect how the crowd is moving. Results from three other musical performances at SoFi in summer 2023 were similar, though differences in the signals may relate to the musical genre and variations in audience motions.

Introduction

Human activities are well-known ambient seismic noise generators (e.g., Diaz et al., 2017). Large rock/pop concerts are one activity that can produce a notable vibration signal and have previously caught seismologists' attention (e.g., Erlingsson and Bodare, 1996; Green and Bowers, 2008; Denton, 2014). "Concert tremor" is typically recorded as extended duration signals with narrowband, harmonic frequency peaks between ~1-10 Hz, though nearby recordings may also include energy at higher frequencies, particularly audible ranges (>20 Hz). The low-frequency signals are broadly similar to harmonic tremor recorded from volcanic and other sources. Although the signals have been definitively associated with concerts, there has been debate about the exact source of the signals, with arguments for the sound system/instruments and for the audience movements. As with other anthropogenic signals, concert tremor also captivates non-scientists, such as the “SwiftQuake” that went viral after a Taylor Swift concert in July 2023 in Seattle, WA (Caplan-Auerbach et al., 2023). The shaking may even affect people living nearby (e.g., Browitt & Walker, 1993).

During the summer of 2023, Swift performed six concerts during 4-10 August (UTC) at SoFi Stadium in Inglewood, CA. Prior to the concert series, we deployed seismic instruments near and within the stadium (Figure 1). These supplemented the permanent seismic stations in the area and provided more detailed recordings. We focused our analysis on Swift’s 5 August (4 August, local time) concert, though the others are all highly similar. We characterized the seismic signals produced by the concert (e.g., Figure 2) and explored the structural response of the stadium to gain insight into the source of the seismic signals and the stadium vibrations. Additionally, we conducted a brief experiment with a speaker system to further investigate the potential source. Lastly, we briefly discuss analysis results from three other popular music acts that also had concerts at the same venue in the summer of 2023 (Morgan Wallen (country), Metallica (metal), and Beyonce (pop/R&B)) to explore potential differences across genres.

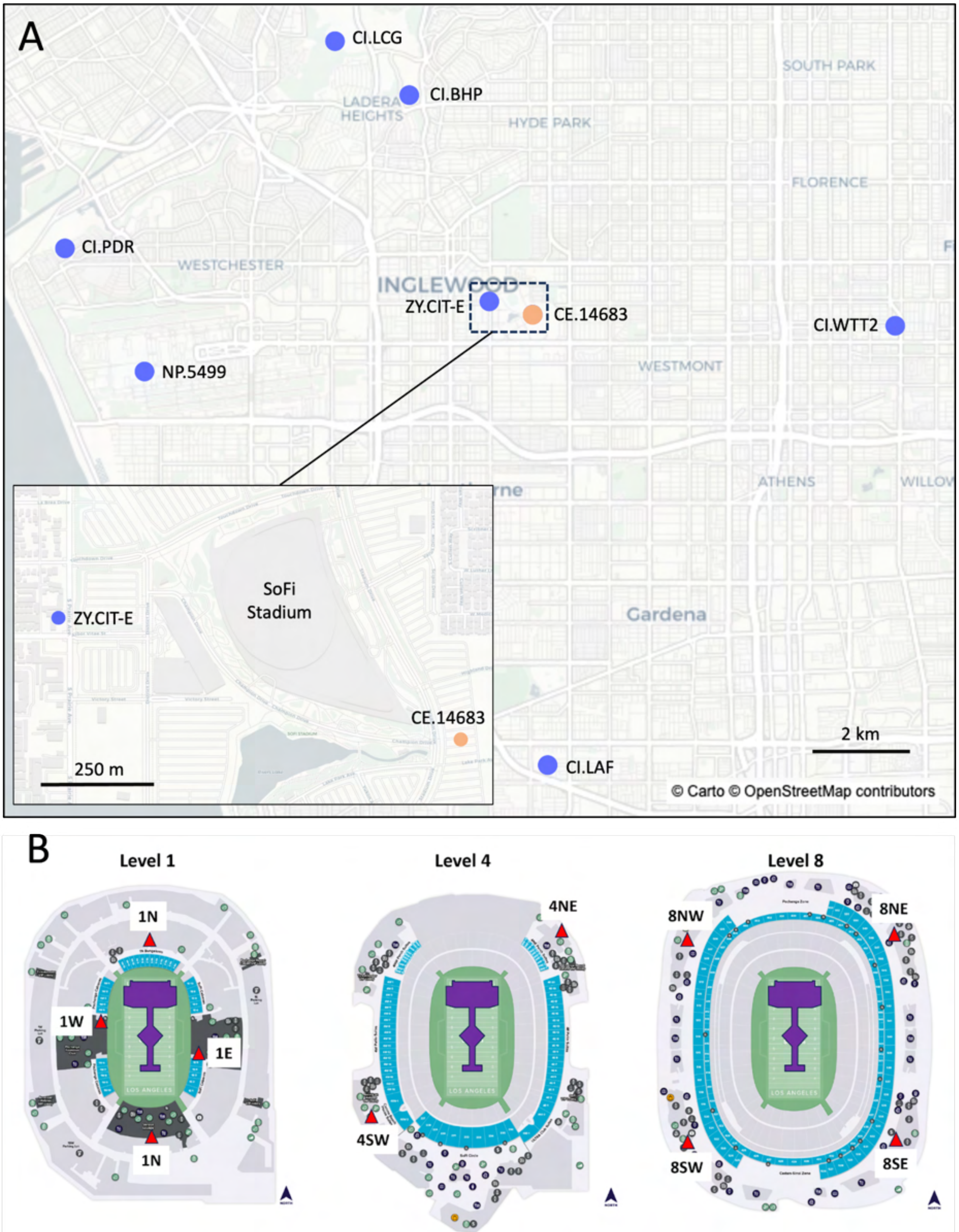
A
CI.LCG
CI.BHP
LADERA HEIGHTS
HYDE PARK
SOUTH PARK
FLORENCE
CI.PDR
WESTCHESTER
INGLEWOOD
ZY.CIT-E
CE.14683
CI.WTT2
WESTMONT
NP.5499
ATHENS
SoFi Stadium
ZY.CIT-E
CE.14683
Gardena
2 km
250 m
CI.LAF
© Carto © OpenStreetMap contributors
B
Level 1
Level 4
Level 8
1N
1W
1E
1N
4NE
4SW
8NW
8NE
8SW
8SE

65

Figure 1: (a) Map showing the concert venue and nearby seismic stations (circles) that recorded signals from the Swift concerts (blue). Zoomed inset shows the location of proximal stations relative to SoFi stadium. (b) Locations of triaxial sensors temporarily deployed inside the SoFi Stadium bowl (red triangles). Purple polygon depicts the concert stage shape and location. Black arrow indicates Stadium-North direction.

Geological and Stadium-Structure Setting

The SoFi Stadium complex is located ~15 km SW of downtown Los Angeles. It overlies thick sediments of varying composition that make up the Los Angeles sedimentary basin and older consolidated rocks that make up the “bedrock” units consisting of deep-water marine deposits at depths of up to 8 km (Yerkes et al., 1965; Wright et al., 1991; Shaw et al., 2015; Ponti et al., 2022). SoFi is located a few kilometers west of the surface location associated with the thickest part of the basin. The geotechnical specifications for the site are “deep alluvium” Class C, with measured Vs30 of ~400 m/s (California Strong Motion Instrumentation Program, CSMIP station No. 14M33). The stadium complex is within the active Newport-Inglewood fault zone, where the main strand is strike-slip and restraining bends formed by steps are dip-slip (Sahakian et al., 2017). The total Newport-Inglewood fault system extends along the western side of the Los Angeles basin for over 60 km and is considered capable of generating M7+ earthquakes (Sahakian et al., 2017).

The SoFi Stadium complex consists of several components, including the stadium bowl containing the field where football games and concerts are held, and an isolated free-standing roof-canopy system. The stadium bowl seats over 70,000 spectators within eight levels for regular events and over 100,000 spectators during special events. Because SoFi is close to Los Angeles International Airport (LAX), the lowest level had to be constructed approximately 100 ft

(30.5 m) below ground level so that the top of the structure would be out of airplane flight path altitudes. Level 6 corresponds to ground level, and the bottom level of the bowl where the field is located is about 100 ft below ground level. The bowl is physically separate from the surrounding mechanically stabilized earth retaining walls encircling the entire bowl and bounding a 12-foot-wide, open-air, oval annulus. SoFi stadium was constructed between 2016 and 2020, and additional structural design details are provided in Supplementary Text S1.

Seismic Data

Signals from the Swift concerts were detected on permanent seismic monitoring sites in the CI (California Institute of Technology, 1926) and NP (U. S. Geological Survey, 1931) networks as well as sensors that were temporarily deployed near and within the stadium prior to the concert series. The network sites consist of strong motion sensors (i.e., accelerometers), sometimes co-located with a seismic broad-band instrument. CI data is typically acquired at 100 Hz sampling and archived at the Southern California Earthquake Data Center (SCEDC, 2013). A strong motion sensor (2G Episensor) and Basalt data logger were temporarily installed ~400 m west of the stadium (ZY.CIT-E, Figure 1a inset). The sensor and data logger were installed on foundation level slabs of a building with good ground coupling, and data was collected at both 100 and 200 Hz sampling rates during 5-10 August (UTC). Additionally, 100 Hz data were obtained from a CE network station located under the SoFi parking lot (~490 m from stadium center) for two Metallica concerts (26 & 28 August) and one Beyonce concert (2 September) (California Geological Survey, 1972).

We also deployed a set of instruments from 4-10 August inside the stadium for the structural response analysis. The sensors are part of the Community Seismic Network (CSN), which consists of about 1200 stations deployed at the ground level and on upper floors of buildings throughout California (Clayton et al., 2020; Kohler et al., 2020). CSN sensors are low-cost

MEMS accelerometers that record acceleration waveform data continuously at 50 Hz sampling within ± 2g maximum amplitude levels. The sensors relay continuous waveform data and shaking intensity parameters using the Amazon Web Services cloud environment. For this study, we placed the triaxial CSN sensors in the stadium as follows: four on Level 1 (lowest level at the same elevation as the concert stage), two on Level 4 (halfway up the stadium bowl), and four on Level 8 (the highest walkable level inside the bowl). The sensors were placed approximately equidistantly on each level (Fig. 1b) with the orthogonal horizontal components oriented parallel to the long axis of the bowl/field ("Stadium-North") and to the short axis of the bowl/field ("Stadium-East"). The Stadium-North orientation is about 25 degrees west of geographical north.

Identifying Concert Tremor in Seismic Data

The Taylor Swift concert tremor signals have unique characteristics that make them easy to identify with a spectrogram. Most notable are harmonic, narrowband signals in the low frequency range around 1-10 Hz that each last a few minutes and have temporally-varying amplitudes (Figure 2). These signals repeat across different nights with high correlation and correspond to different songs that were played (Table S1). Additionally, the signals were very similar to those recorded outside Lumen Field in Seattle, WA, during Swift concerts one month before the SoFi concerts (Caplan-Auerbach et al., 2023). Because each night is not exactly repeated, temporal shifts between songs and for the concert as a whole are observed (Figure S1) as well as two surprise songs that differed every concert (songs 37 & 38 in Table S1). The signals were clearly recorded on stations located up to ~9.5 km from the stadium, including a strong-motion station located at LAX (NP.5499). The recorded signals were similar on all three sensor components, although the relative amplitudes differed for each signal.

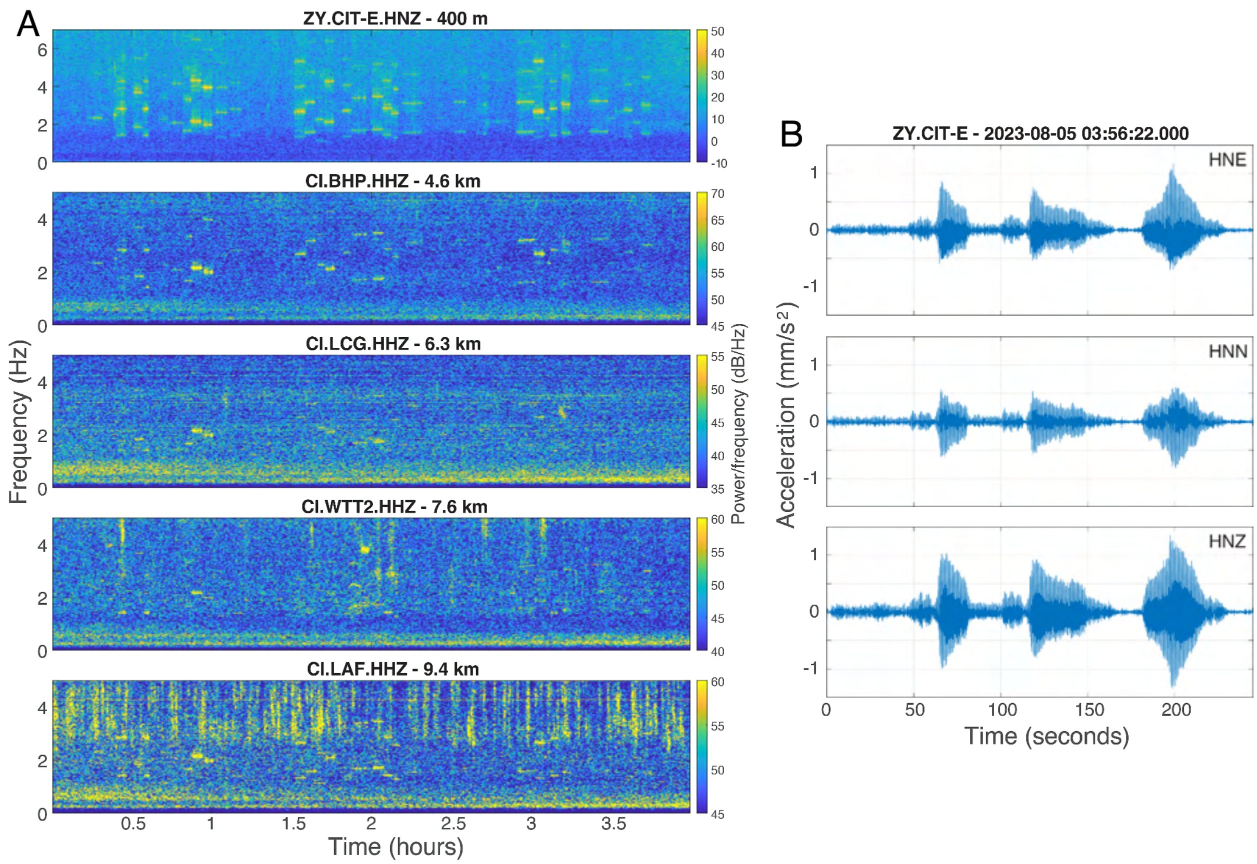

Figure 2: (a) Vertical-component spectrograms from five stations at varying distances for four hours around the 5 August 2023 Swift concert (starting at 03:00 UTC, or 8pm on 4 August, local time). (b) Example concert tremor waveform for song 9 ("Love Story"), bandpass filtered from 1-6 Hz.

Concert Tremor Characterization & Relation to Songs

To analyze the concert tremor in more detail, we first obtained the start and end times of each signal. Since the signals have well-defined frequency bands, we used the Hough transform approach (Hough, 1962) to find lines in the spectrogram. The spectrograms were generated for a 4-hour window around the concert time using windows of 8192 samples for 100 Hz data (e.g., CI.BHP) and 16384 samples for 200 Hz data (e.g., ZY.CIT-E), both with 90% overlap.

To make the spectrograms more suitable for applying the Hough transform, we needed to improve the signal-to-noise ratio as much as possible and then binarize the image. For stations with signals that were well-recorded on all three components at the same frequencies, we stacked the spectrograms to strengthen signals and reduce noise; otherwise, we used the vertical component, which typically had the best signal-to-noise ratio. We then normalized the spectrograms, either by dividing by the maximum value of the entire spectrogram or by the maximum value of each column (i.e., time window). The latter approach led to better balance between the strongest and weakest signals and worked best in situations where amplitudes varied significantly between songs, such as on station ZY.CIT-E. The normalized spectrogram was then turned into a binary image (i.e., values of one and zero) using either an adaptive method or a minimum threshold value (Figure 3).

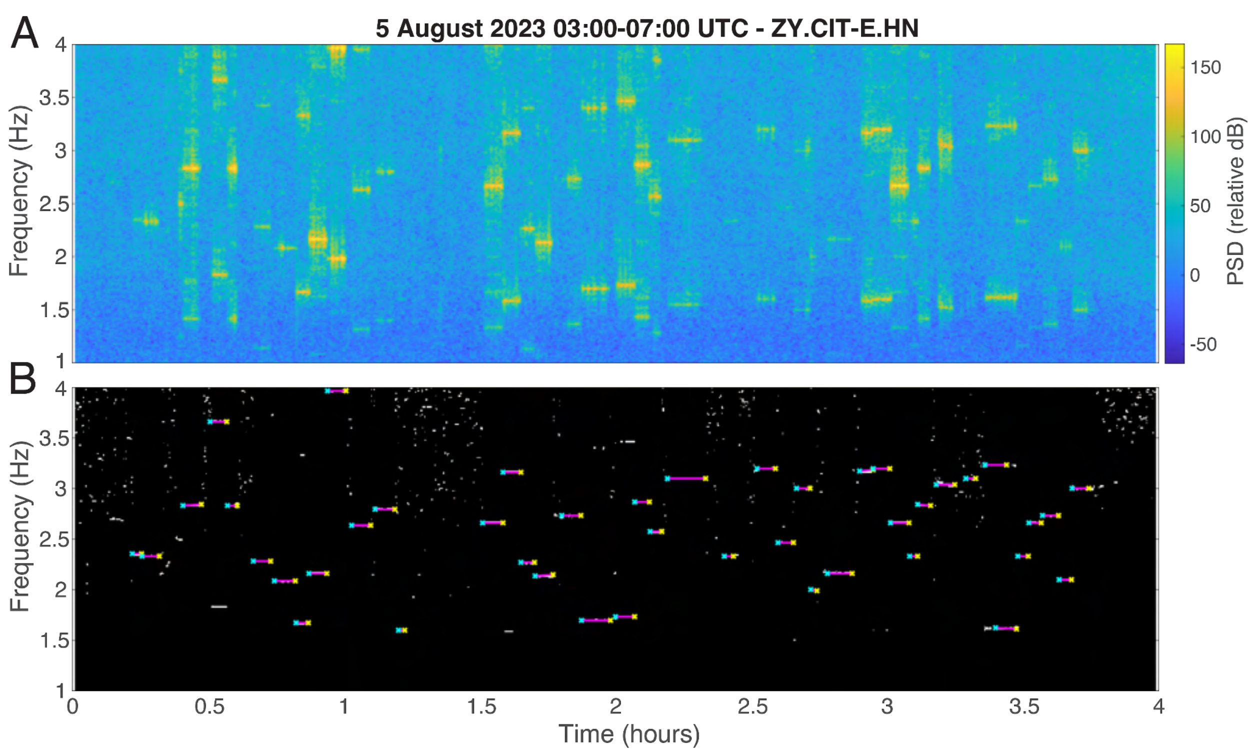

Figure 3: a) Preprocessed spectrogram using a 3-channel stack and column-based normalization. b) Binarized spectrogram based on a minimum threshold and the final set of Hough lines (magenta lines with cyan and yellow x's at end points).

Once a binary image was generated, we used the Hough transform approach (Hough, 1962) to identify lines in the image. The Hough transform parameterizes a line using two variables: the length of a vector starting at the origin and meeting the line perpendicularly (ρ), and the angle of that vector from the x-axis (θ). After its application, we searched the resulting ρ-θ space for peaks that potentially corresponded to line segments in the image. We filtered the list of line segments to remove duplicates and extraneous lines using *a priori* knowledge that our signals are horizontal or nearly so and should correspond to one line per song (temporal constraint). A few manual corrections were made for trickier situations (e.g., combining overlapping lines). We determined the signal durations from the end points of the lines and estimated the frequencies from the lines' vertical positions. The start times and durations of the lines were used to extract seismic data for each song. We calculated the spectrum of the signal and identified the frequency peak(s) with more precision using an automatic function along with manual intervention when necessary to remove peaks from strong noise while retaining weaker signals.

We matched our list of spectrogram lines with songs in the concert's setlist (obtained from https://www.setlist.fm, last accessed 30 Oct 2023). By using the line start times, durations, and frequencies, we were able to match the lines with the associated songs, even though some songs were missing from the seismic data. This is similar to previous studies (e.g., Denton, 2014) that have found a correlation between a song's beat rate and the frequency content of the associated seismic signal.

For the 5 August Swift concert, we were able to detect 43 of the 45 songs plus a weak signal during the introductory recording played on the sound system (0 in Table S1). Two adjacent songs (30 & 31) with the same beat rate per minute (BPM) were likely merged into one Hough line, so we associate both with the same line. Two other songs (39 & 40) had a similar situation, though the signal was split into two overlapping Hough lines. The two songs missing from our analysis were not visible in the ZY.CIT-E spectrogram and likely did not create a signal above the noise floor for that site and distance.

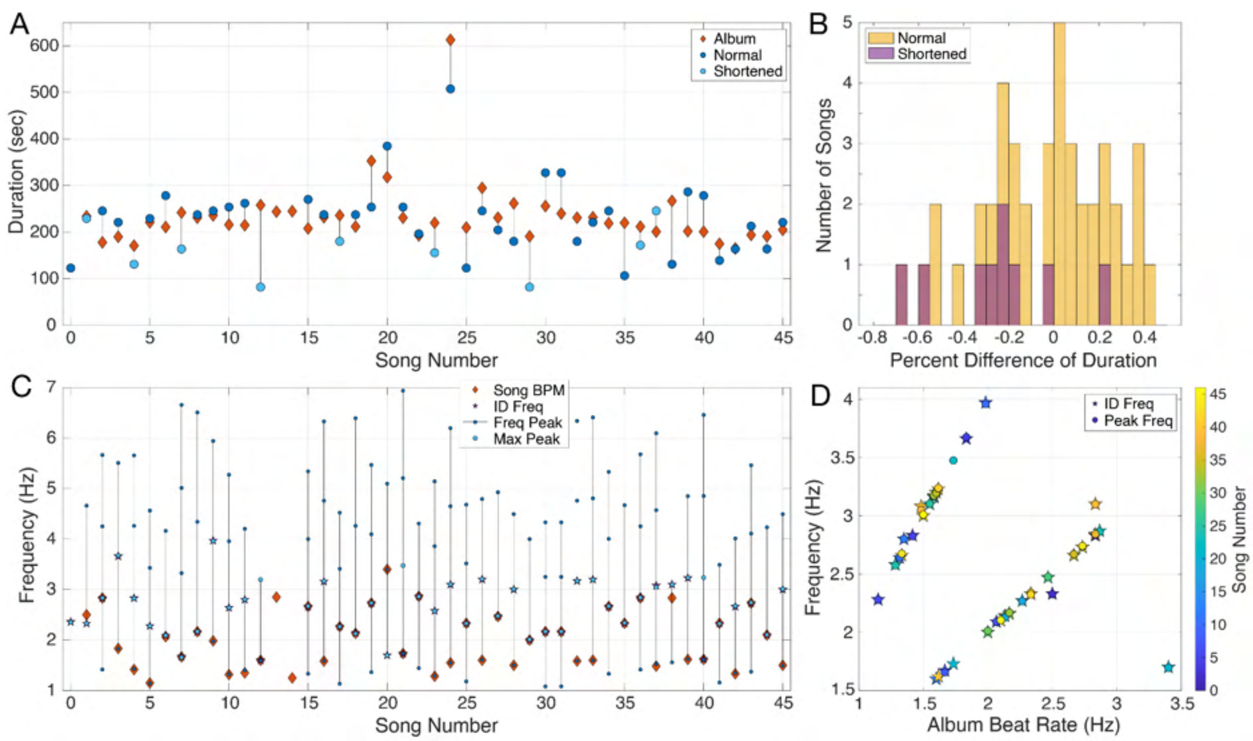

Figure 4: a) Album and seismic duration of each song in chronological order. “Shortened” refers to songs that were marked as such in the set list, and “normal” refers to the rest. b) Histogram of the percent difference between the seismic duration compared to the album duration. c) Album beats per minute (BPM, red diamonds), the frequency at which the Hough line was identified

(magenta star), and frequency peaks from the spectrum (blue circles, lighter blue for the strongest peak) for each song in chronological order. d) Comparison of the album beat rates to the identification frequency (stars) and frequency peaks (circles). “Song number” refers to the index in Table S1.

After matching the signals and songs, we compared the duration and beat rate from the album version (i.e., studio recording) of the song, keeping in mind that live songs are not always played exactly the same as the album versions. Both values were obtained from https://songbpm.com (last accessed 30 Oct 2023). Differences between the album and seismic durations varied from 0.7% to 68%. Nine of the 44 songs were marked as “shortened” on the setlist, and most of these had seismic durations shorter than the album version (Figure 4a&b). For the rest of the songs, 22 of 36 seismic durations were within 25% of the album duration, and 30 of 36 were within 40%.

The album version beat rates and the frequencies of the seismic signals match very well. Nearly all songs correspond to a maximum frequency peak approximately equal to or double the beat rate (Figure 4c&d). The only song with a beat rate above 3 Hz (180 BPM) had a maximum frequency peak at half the rate. We found up to 4 frequency peaks per song at integer ratios, indicating the signal is harmonic. All but three songs were identified at their strongest frequency peak (i.e., harmonic).

Particle Motion

We further explored the nature of the seismic signals by considering the particle motion (e.g., Figure 5a & S2), which provides information about the type of wave generated and may give insight into the source. For easier comparison, we parameterized the particle motion of each song and harmonic (frequency peak +/- 0.2 Hz) on station ZY.CIT-E using moving windows over the song's duration with the median values for each song and harmonic presented in Figure 5b (e.g., Montalbetti and Kanasewich, 1970; Ereditato and Luongo, 1994; Thompson and Reyes, 2017). The window lengths were determined based on the waveform duration. The strongest harmonics of each song typically have a flat, elliptical motion (planarity>0.85 and rectilinearity between 0.4 and 0.9) similar to a Rayleigh wave, though the directionality (i.e., azimuth, inclination) varies for each song and harmonic and sometimes even within a song. Most exceptions to this are songs with weaker signals that are more likely to be affected by noise. Other harmonics that are relatively weak but with good signal-to-noise typically show a complex particle motion that greatly varies through time (e.g., Figure S2) and isn't well described by the parameters in Figure 5b. The inclination of the elliptical motion and complex motions of higher harmonics could result from interference between Rayleigh waves and scattered body waves in the basin (e.g., Ma et al., 2016). For the signals that were well-recorded by CI.BHP, we observed similar planar, elliptical particle motions.

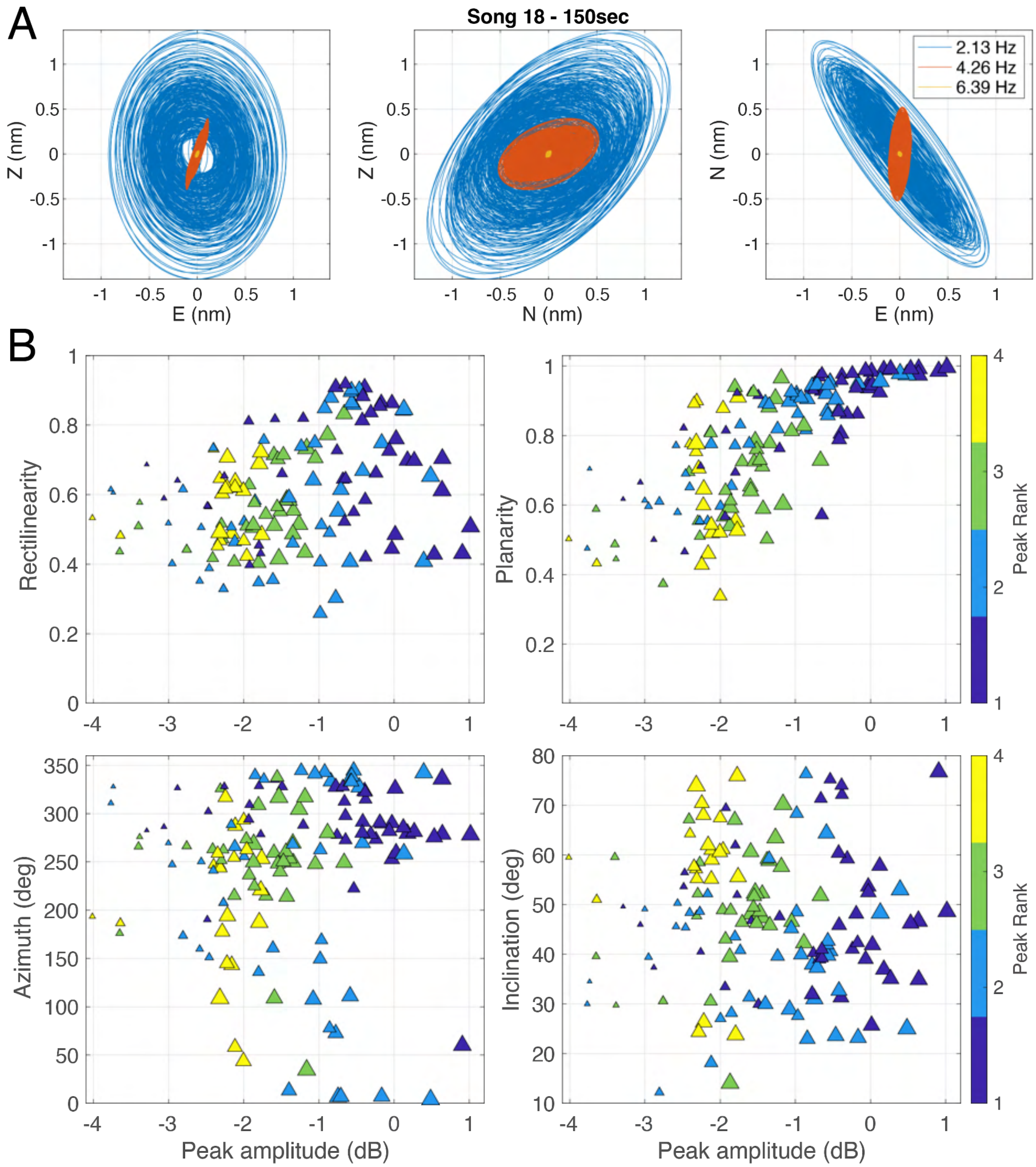

Figure 5: (a) Displacement particle motion of each harmonic at station ZY.CIT-E (Z, N, E components) for the first 150 seconds of song 18 (Table S1). Data were bandpass filtered between +/-0.2 Hz of the frequency peak. (b) Median values of parameters describing particle motion for each harmonic plotted against the harmonic's amplitude measured from the power

spectrum of the acceleration waveform from ZY.CIT-E.HNZ. Colors show the ranking of the harmonic with 1 being the strongest for each song. Marker size reflects the M_{Le} of the song.

Determining the Strength of Concert Tremor

When engaging with the public about ground-shaking events, everyone wants to know "how big was it?" Seismologists have established methods for determining the strength of earthquakes, the most well-known being magnitude. For atypical signals, however, this question is more complex. Is a magnitude derived from the peak amplitude meaningful for a concert tremor signal that's a few minutes long? For this reason, other measures of strength have been introduced, such as reduced displacement for volcanic explosion tremor (e.g., Aki and Koyanagi, 1981).

Earthquakes produce permanent deformation, and the moment magnitude traditionally computed from seismic moment is a measure of the deformation. Concert tremor, however, is a transient phenomenon that does not leave permanent deformation, so the best evaluation of signal strength should be radiated energy. If the estimate is based only on the largest amplitude, the magnitude of the concert tremor would approximate the energy radiated during a brief energetic time span. Alternatively, one can calculate the energy radiated during the entire song and then interpret it in terms of the magnitude of an earthquake that would have radiated the same energy. Such an estimate of the song strength is more representative of the energy released during a performance.

Radiated Energy

We first calculated the radiated energy, E_R, and equivalent local magnitude, M_L, for songs performed during the 5 August concert and recorded by the temporary strong-motion sensor, ZY.CIT-E (Fig. 1a). To prepare the seismic data for processing, we bandpass filtered acceleration waveforms within 1-6 Hz and deconvolved the instrument response to obtain ground velocity in cm/s.

Following Kanamori et al. (1993), we computed E_R as proportional to the time-domain integration of the squared ground-motion velocity ν, rotated into radial (R), transverse (T), and vertical (V) components:

$$E_R = 4\pi r^2 * \rho\beta * \int_{t1}^{t2} \nu^2 dt \qquad \text{(Eq. 1)}$$

$$\nu^2 = \nu_R^2 + \nu_T^2 + \nu_V^2 \qquad \text{(Eq. 2)}$$

where r is the propagation distance (400 m), ρ is the ground density (2500 kg/m^3), β is the wave propagation velocity (350 m/s), and *t1* and *t2* are the start and end of the songs, respectively (e.g., Figure 3b). Note that Kanamori et al. (1993) used S-wave velocity since S waves carry most of the energy of local earthquakes, but our signals are predominately Rayleigh waves. The choice of phases, however, does not change the equation since we are estimating the energy of a local event as a whole, which depends on the phases that carry most of the wave energy. Because of the seismic station proximity, we assumed a uniform half-space, where the Rayleigh waves are non-dispersive with a constant phase velocity of ~90% of the shear-wave velocity, determined from Vs30 velocities for the concert venue location. The final E_R computation requires a correction for attenuation *Q*, site response *SR*, and radiation pattern *R:*

$$E_{RT} = C(Q, SR, R) * E_R \qquad \text{(Eq. 3)}$$

Following Kanamori et al. (1993), we assumed the attenuation from Jennings and Kanamori (1983), average radiation pattern equal to 1, and an amplification factor of 2 for the station, resulting in factor C(Q, SR, R) equal to 0.0625. Finally, we computed the corresponding equivalent M_L from:

$$\log E_{RT} = 1.96 M_L + 9.05 \qquad \text{(Eq. 4)}$$

where E_{RT} is in ergs.

The radiated energy per song varies over three orders of magnitude, with equivalent M_L ranging from -0.5 to 0.85 (Figure 6). We also examined energy per minute, which is a more informative way to discuss and compare the strength of individual concert tremor signals as well as non-seismic and seismic signals since durations can greatly differ. The per song and per minute energy rankings generally correlate with each other, although not exactly (Tables 1&S1, Figure 6a). The first half, and especially the first quarter, of the concert was more energetic, with the exception of song 34, and there is no apparent correlation between E_R/min and song beat rate (Figure 6c). While the most energetic songs have an equivalent M_L of 0.85, their minutes-long durations are much greater than the <~1 second durations of similar magnitude earthquakes. For comparison, the strongest concert tremor magnitude averages ~0.007 M_L/sec, about 120 times less than an M_L 0.85 earthquake.

Table 1: Radiated energy E_R in Joules and equivalent local magnitude M_L per song duration and per minute for the top 5 most "energetic" signals. The numbers in parentheses refer to song ranking based on E_R(J)/song sorting. The values for all songs can be found in Supplemental Table S1.

song	**ER(J)/song**	**ER(J)/min**	**ML/song**	**ML/min**
34. Shake It Off	5210 (1)	1270 (2)	0.851 (1)	0.208 (3)
8. You Belong With Me	5170 (2)	1310 (1)	0.849 (2)	0.214 (2)
9. Love Story	4150 (3)	1010 (3)	0.800 (3)	0.195 (4)
2. Cruel Summer	3180 (4)	775 (5)	0.741 (4)	0.181 (6)
21. 22	2060 (5)	486 (7)	0.645 (5)	0.152 (9)

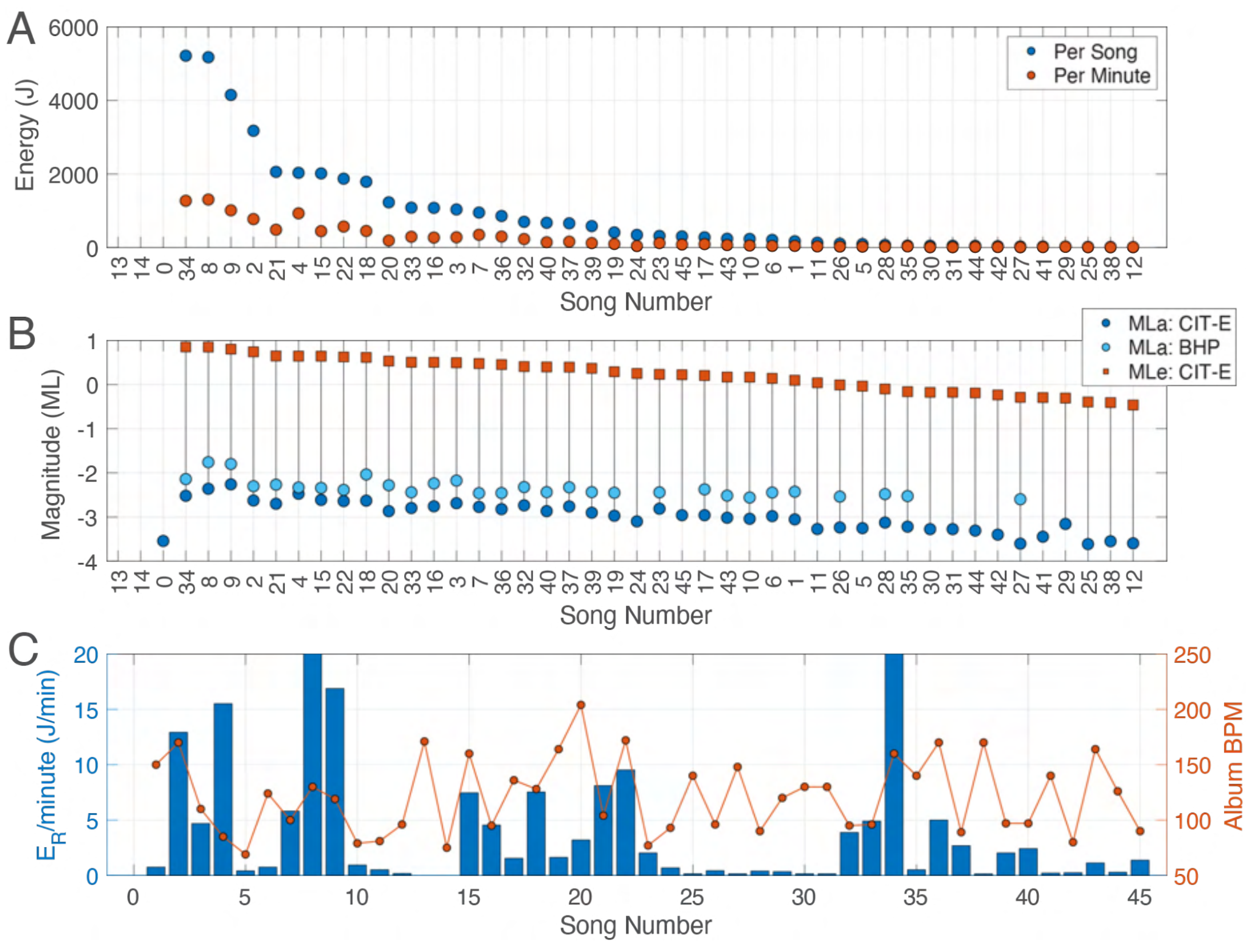

Figure 6: a) Radiated energy for each song, per minute and per song. b) Comparison of local magnitude (M_L) per song computed from energy (red squares) and peak amplitude (circles) as detailed in the text. c) Radiated energy E_R per minute for each song in chronological order compared to song beat rate from the album recording. “Song number” refers to the index in Table S1.

Local Magnitude from Peak Amplitude

For comparison, we also calculated the M_L of the concert tremor with the traditional method using peak amplitude (Richter, 1935). Waveforms were filtered to isolate the signal and reduce noise as much as possible. We chose a 1-6 Hz filter for station ZY.CIT-E and a 1.5-3.5 Hz filter for station CI.BHP and used the vertical component (HNZ and HHZ, respectively). Since the frequency range corresponds to the flat part of the instrument responses, we simply used the sensitivity value to convert to physical units. The peak amplitude was measured as the maximum absolute value of the displacement waveform with the first and last four seconds removed to avoid integration artifacts. We used the Kanamori et al. (1993) form of the local magnitude equation with constants determined for Southern California (Hutton et al., 2010):

$$M_L = \log_{10} A + 1.14 \log_{10} r + 0.002193\, r + 0.4985 \quad \text{(Eq. 5)}$$

where A is the peak amplitude in mm and r is the distance in km. A site correction is typically also included but is ignored here since the temporary station ZY.CIT-E does not have one and it would only shift the values up or down. For reference, station CI.BHP normally has a correction of -0.3.

The amplitude-based magnitude (M_{La}) estimates are much smaller than those based on energy (M_{Le}) (Figure 6b), consistent with the expectation for a long-duration tremor signal. While the songs with higher M_{Le} tend to also have a higher M_{La}, the ordering is not one-to-one, even for M_{Le}/min. Differences in the two M_{La} estimates may be related to site effects that are not accounted for and/or the different frequency bands that were recorded and used.

Structural Response of the Stadium

Strong-motion CSN sensors were deployed inside the stadium to verify the sources of vibrations observed outside stadium grounds. During the concerts, the CSN sensors recorded acceleration signals with good signal-to-noise on the upper levels. The waveforms in all three components exhibit amplification in the higher elevation levels (Figure 7). The maximum acceleration was about 1%g recorded in the Stadium-East and vertical directions on Level 8SW. The horizontal motions, particularly in the Stadium-East direction, were about as large as the vertical motions, indicating a significant amount of horizontal structural response throughout the concerts.

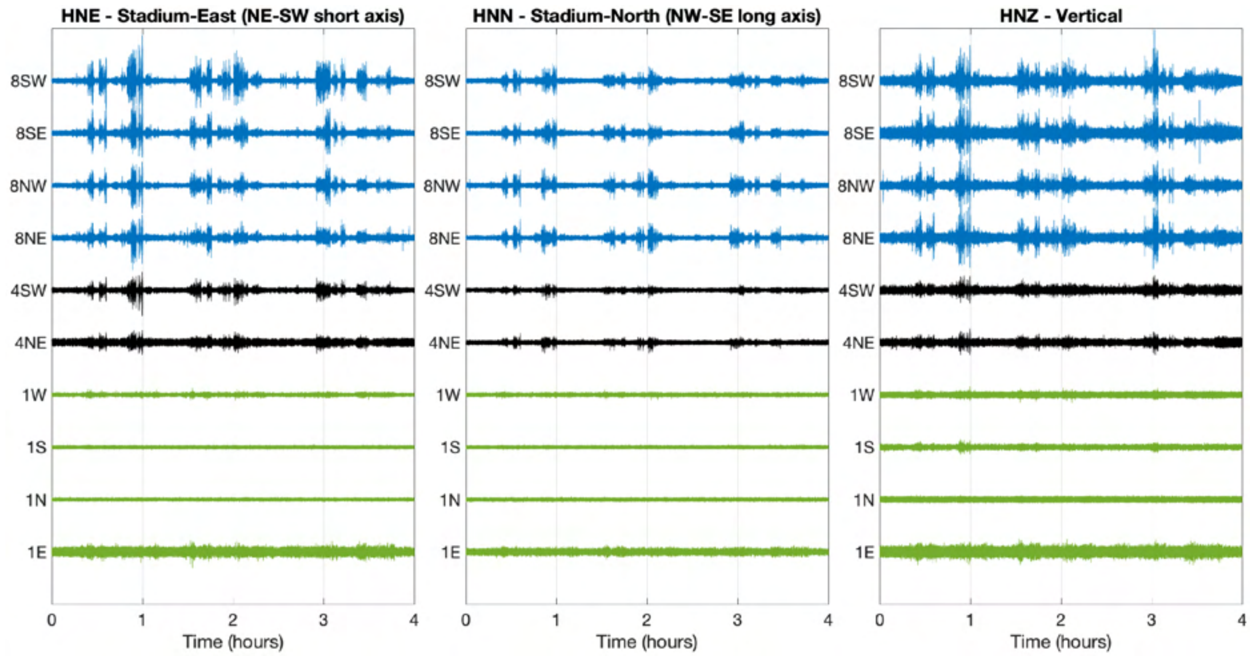

Figure 7: Unfiltered accelerations recorded on strong-motion CSN sensors inside the SoFi stadium bowl for the concert starting at 03:00 on 5 August 2023 (8pm on 4 August, local time). Sensor locations are indicated on the left side of each waveform. Colors group sensors by bowl level. All waveforms are normalized by the same constant to retain their relative amplitudes.

Spectrograms of the stadium station data (Figure 8) exhibit high spectral energy at the same frequencies throughout the concerts as the network stations (e.g., Figure 2a), suggesting the stadium motion has largely the same source as the vibrations recorded on the sensors external to the stadium. Stadium vibrations are likely a complicated mix of concert-induced frequencies and stadium modal frequencies (“structural modes”), within the same frequency range (Catbas et al., 2010). If there are fundamental resonant bowl modes below 1 Hz as expected, they are not excited during the concert, as the lowest recorded harmonics in the spectrograms are above 1 Hz (Figure 8).

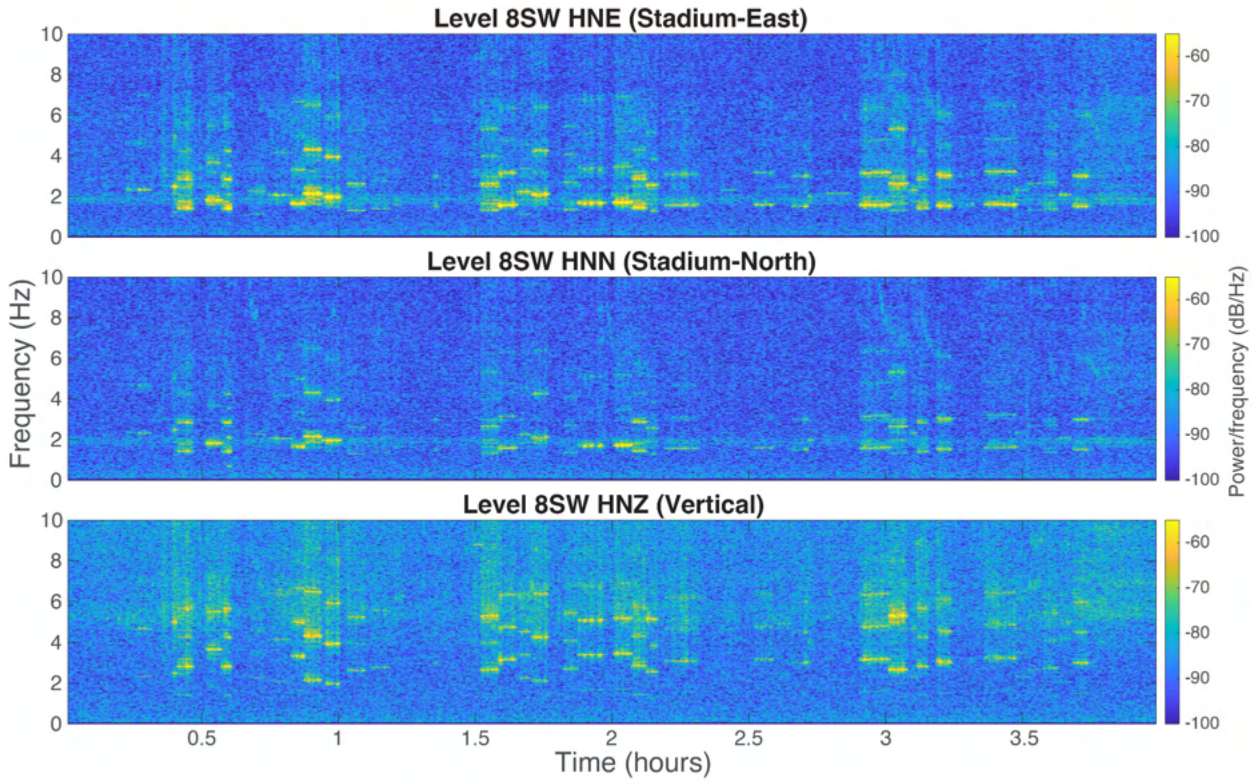

Figure 8: Spectrograms from 4 hours of data recorded by Level 8SW CSN sensor for the concert starting at 03:00 on 5 August 2023 (8pm on 4 August, local time) produced using 4096 samples per window with 90% overlap.

What Generates Concert Tremor?

The source of low-frequency concert tremor signals has been debated, particularly whether they are produced by the synchronized movement of the crowd or by the sound system and/or instruments coupled to the stage. Previous studies of concerts at stadiums (Erlingsson and Bodare, 1996) and outdoor festivals (Denton, 2014) have argued for a crowd-based source. It's known that both individuals and crowds can synchronize their movements to a beat (e.g., Styns et al., 2007; Solberg and Jensenius, 2019) and that those movements can produce large amounts of vibrational energy (e.g., Chen et al., 2019). Malone et al. (2015) found similar narrowband, harmonic seismic tremor from a chanting crowd during a football game, indicating that crowds are capable of generating such signals since no music would have been playing in that situation. In contrast, Bowers and Green (2008) argued that the low-frequency seismic signals observed from an outdoor electronic dance music festival were generated by vibrations from the sound system in response to the musical beat.

Regardless of source, studies typically ascribe the low-frequency signals to the Dirac comb effect, wherein a series of repetitive impulsive signals functions as a single coherent signal. A spectrogram of a Dirac comb reflects the rate of the repetitive signal rather than the spectrum of each individual signal. For a speaker or instrument source, the low-frequency signal would be generated by vibrations of the speakers themselves and/or the concert stage (or building structure) that are generated in response to the song’s beat. In this case, music with a strong repetitive beat, likely from the rhythm instruments (e.g., bass guitar, drums), should produce a stronger, steadier signal compared to music that is missing these components (e.g., guitar-only song). For a crowd-based source, the movements of the crowd (e.g., jumping, swaying) to the beat would release energy directly into the ground and/or induce vibrations in the building structure.

To test the source hypotheses in a controlled setting, we conducted a simple experiment to record music played on a portable public announcement speaker system with the same strong-motion sensors used for our temporary deployment (see details in Supplemental Text S2). One sensor each was placed in front of and behind the speaker system at 1 m distance with the north component parallel to the speaker system. We played the Swift song “Love Story” (song 9, 119 BPM), and during the last chorus, one person repeatedly jumped with the beat near the speaker. At maximum volume, vibrations from the speaker were clearly felt while standing next to it. We also tested a steady beat (120 BPM) from a bass guitar to isolate the signal of a single instrument playing the most basic rhythm. Clear, harmonic, low-frequency signals were recorded only during the jumping, though higher-frequency energy (~50-90 Hz) was recorded during the music-only and bass-beat tests (Figure 9). The fundamental harmonic from the jumping was ~2 Hz, consistent with the beat rate of the song.

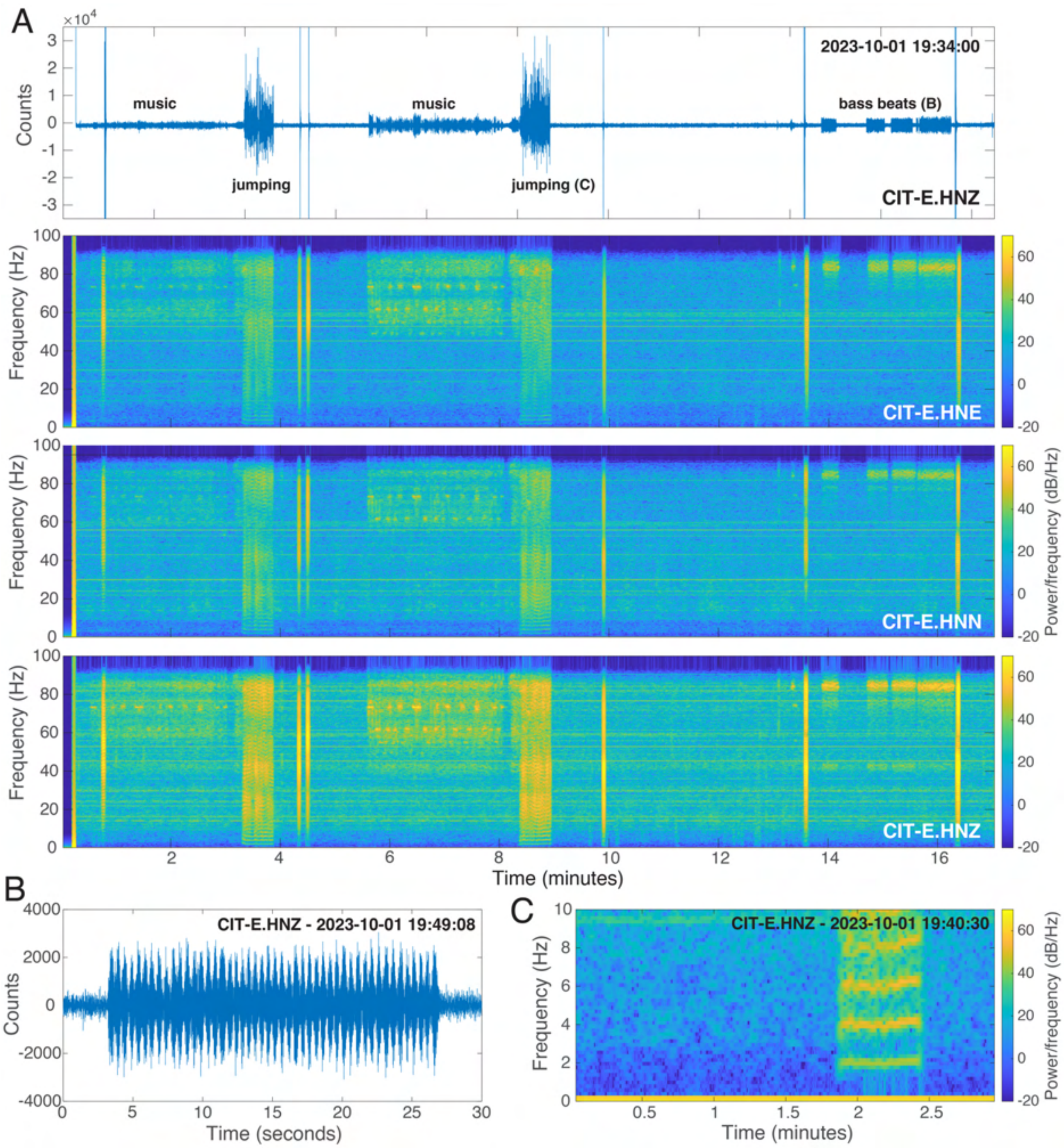

Figure 9: (a) Strong-motion recording from the speaker experiment. Spectrograms produced using 1024-sample windows with 90% overlap. The sharp broadband lines were strong jumps that marked the start and end of a test. (b) Expanded waveform of one bass-beat test to better show the repetitive beat. (c) Expanded spectrogram of the low frequencies from the second jumping test.

Overall, the evidence suggests that crowd-movement is the primary source of the low-frequency signals, with the speaker system or instruments potentially contributing via stage or building vibrations. Our experiment showed no low-frequency signal from even a basic, steady bass beat, but the signal did appear for someone bouncing with the music. The difference may be in the character of the signal - compared to the sharp spikes of the jumps, the bass beats have a rounder, more emergent envelope that may not effectively function as a Dirac comb. One caveat is that our experiment did not include a stage or stadium-grade sound system, so we cannot completely rule out speakers as a vibrational energy source. However, there are other aspects from the concert data analyses that also support a dominantly audience-based source. First, the opening act for the Swift concerts was only possibly recorded on one or two nights (Figure S1), although the artist performing right before Swift was the same every night and the sound system should also have been the same. Second, during concert tours, the crew typically performs sound checks and/or practice runs prior to the event. We did not observe seismic signals from these checks. Similarly, Caplan-Auerbach at al. (2023) found no low frequency signals recorded during sound checks from the 2023 Swift concerts in Seattle, WA, but did find higher frequency signals comparable to those during the concert. Third, changes in the particle motion between and within songs would not be expected from a consistent, static speaker system but could be generated by changing crowd motion. Fourth, low-frequency signals were observed during songs that do not have a strong musical beat (e.g., songs 37, 38), which would not be expected if the speakers were the primary source. Fifth, the strongest harmonics are mostly between ~90 and ~200 BPM (Figure 4d) regardless of the song's beat rate, which is consistent with the 1.5-3 Hz frequency band (90-180 BPM) previously determined for loads induced by people jumping to a beat (Sahlin, 1986 via Erlingsson and Bodare, 1996). As a final note, the decrease in energy release over the concert duration may potentially relate to the audience getting tired as the beat rates don't reflect a systematic change in the type of song played (Figure 6c).

Another aspect of the source to consider is the generated particle motions. For one person jumping in our experiment, the particle motion was approximately linear and nearly vertical, as would be expected for a downward-force point source (Figure S3). However, the particle motion of the dominant harmonics is planar-elliptical, similar to Rayleigh waves, as has been noted in other studies (e.g., Denton, 2014). Since a stadium crowd is distributed over the footprint of the bowl, it cannot be taken as a point source for the close station distances. Additionally, concert crowds don't necessarily all jump together. During a large stadium concert, Erlingsson and Bodare (1996) noted that the crowd moved in a ripple or wave-like motion that initiated near the stage and propagated outward with the sound, rather than in a single coordinated jump. The planar, elliptical motion may reflect the distributed point sources (i.e., people) moving as a rolling wave. This ripple effect could also explain the typically stronger east or stadium-east component signals (perpendicular to the extended stage setup) within and outside the stadium.

Similar to particle motion, the stadium response itself shows approximately equal shaking intensity in the east and vertical directions, with lower yet notable shaking in the north direction. If the audience motions are the source of both vertical and horizontal forces, this could be explained by different mechanisms occurring at the same time. One obvious source for vertical loading is individual and collective audience participants jumping up and down. Lateral variations in audience response (e.g., wave-like movement, subsections of the crowd jumping) could result in moments being applied to particular stadium levels, which could result in horizontal components of force. Individual audience motions could also involve moving laterally (e.g., swaying motion) against the concrete seat framing system.

Vibrational energy generated by activities inside the stadium is transmitted into the underlying soil and to locations outside the stadium through soil-foundation coupling at the bottom of the bowl. The SoFi foundation consists of reinforced concrete pile caps (thick, continuous, horizontal mats), supported by concrete piles extending vertically into deeper ground. The piles are isolated from the surrounding soil and sit on concrete footings (CSMIP Station No. 14M33); this is the system that carries the load of the superstructure. The sources of vibrational energy are the vertical and horizontal forces produced inside the stadium and its structural systems. Because it does not come into contact with the surrounding retaining walls or with the column-canopy system, the stadium bowl directs the loading forces into the underlying soil directly through the foundation system.

Comparison to Other Musical Acts

We conducted the same analyses for concerts from three other musical acts that performed at SoFi stadium in summer 2023: Morgan Wallen (country) on 23 July, Metallica (metal) on 26 & 28 August, and Beyonce (pop/R&B) during 2-5 September (all UTC). Additionally, we observed clear signals on station CE.14683 (Figure 1) from three well-known opening acts (Pantera on 26 August, Five Finger Death Punch on 28 August, and DJ Khaled on 2 September). Overall, the results from these concerts are similar to those from the Swift concerts (Figures 10&S4-6, Supplementary Tables S2-4) and support the audience-source hypothesis. For station

CE.14683, the strongest frequencies tended to be on the second harmonic (i.e., double the beat rate), which may be an effect of the instrument or site response. Interestingly, signals from the Metallica concerts were not as neatly peaked or consistent in frequency as any of the other analyzed concerts. While searching for information about those concerts, we came across several comments and forums that mentioned poor sound quality, especially in the higher bowl levels. If fans had a hard time discerning the song or beat, it may explain the more variable signals, as it would have influenced their movements. Other possibilities are that metal bands in general tend to play “in the moment” and are less likely to stick to a beat (or an album recording) compared to the highly choreographed shows of Swift and Beyonce, or that metal fans may move in a manner that’s less amenable to generating steady vibrations.

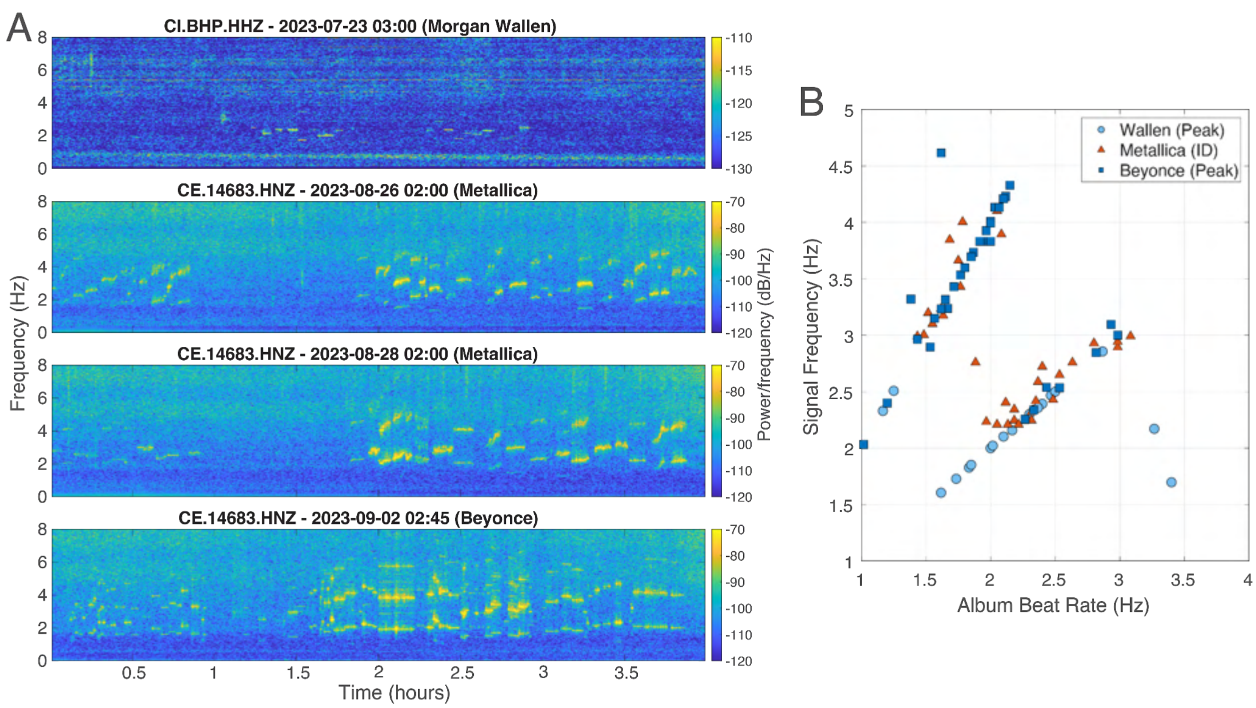

Figure 10: a) Spectrograms from the analyzed Morgan Wallen, Metallica, and Beyonce concerts. Note that Metallica had a different setlist each night and is shown twice. Signals from opening acts are visible during the first hour of the CE.14683 recordings. b) Comparison of signal frequency and song beat rate for all concerts shown in (a), not including opening acts.

The identification frequency was used for the Metallica concerts instead of peak frequency due to effects of the broader-band signals on the peak detection.

Summary

Large concerts and music festivals are known to produce seismic signals, though there has been debate about the source of the low-frequency harmonics associated with those signals. In this study, we analyzed 43 of 45 songs from a Taylor Swift concert that were seismically recorded on permanent network stations and temporary stations near and within the stadium where she performed. We found a strong relation between the frequency of the harmonics and the song beat rate, similar to previous studies, whereas there was up to 60% difference in seismic and album recording durations. The particle motions of the strongest harmonics were consistent with Rayleigh waves, likely with influence from scattered body waves in the basin. Our estimates of signal magnitude significantly differed based on energy release (roughly -0.5 to 0.9) or peak amplitude (roughly -3.5 to -1.7), which is expected for signals with extended durations. Fundamental stadium resonant modes were not observed, and more detailed analysis would be required to determine potential stadium contributions from higher modes. Analyses of concerts from three other genres showed similar results.

Based on the available evidence, we interpreted the seismic waves as resulting primarily from crowd movements to the music. To independently evaluate the source, we conducted a brief experiment with a speaker system and found that only a jumping person was able to produce the low-frequency signals. The music or a simple bass beat played through the speaker only produced signals at high frequencies (~40+ Hz). Since a person jumping produces linear, vertical particle motion, the Rayleigh-wave motion may be generated by the crowd movements occurring in a rolling-wave motion rather than as a single, coherent, coordinated motion. Such variations in movements could also explain the similar amplitudes recorded on the vertical and horizontal components of the sensors inside the stadium.

Data & Resources

The Hough line and frequency peak analyses were done using built-in functions in Matlab. These analyses as well as the particle motion analysis also used the GISMO toolbox for Matlab (https://github.com/geoscience-community-codes/GISMO). For the energy analysis, waveform processing was done with the Seismic Analysis Code (SAC) using SEED volume instrument response (RESP) files. Waveform data and metadata for the CI & NP network stations and the temporary ZY.CIT-E station can be accessed through the Southern California Earthquake Data Center (SCEDC). Per CSN policy through agreements with sensor hosts, non-earthquake data (i.e., from the stadium sensors) cannot be released to the public. Structural and geotechnical CSMIP data are from www.strongmotioncenter.org, Station No. 14M33. The station map was created using Plotly Express and map data contributed by Carto and OpenStreetMap. Supplemental Material includes more details about the stadium construction and speaker experiment, additional figures, the concert analysis data tables, and the speaker experiment waveform data.

Acknowledgements

We thank Hiroo Kanamori for helpful discussions about energy and magnitude, Jackie Caplan-Auerbach for interesting discussions about the concert signals, Jim Meyer for very detailed information about stadium concert sound systems, and Rafael Sabelli and Mark Waggoner for useful information about stadium structural response parameters. We also appreciate helpful comments from [reviewers]. We thank Dave Branum for retrieving data from the CE station that is usually only archived for triggered events. The Southern California Seismic Network (G.T. and I.S.) is funded by the U.S. Geological Survey (USGS) and the California Office of Emergency Management, the latter of which motivated interest for this study. We thank the California Geological Survey, the Terrestrial Hazard Observation and Reporting (THOR) Center at Caltech, and the Divisions of Geological and Planetary Science, and Engineering and Applied Science at Caltech for funding research connected with the Community Seismic Network. The SCEDC is funded through USGS Grant G10AP00091 and the Southern California Earthquake Center, which is funded by NSF Cooperative Agreement EAR-0529922 and USGS Cooperative Agreement 07HQAG0008.

References

Aki, K., and R. Koyanagi (1981). Deep volcanic tremor and magma ascent mechanism under Kilauea, Hawaii. *Journal of Geophysical Research: Solid Earth*, *86*(B8), 7095-7109.

Browitt, C. W. A., and A. B. Walker (1993). BGS Seismic Monitoring and Information Service, Fourth Annual Report. British Geological Survey Technical Report WL/93/08.

California Geological Survey. (1972). *California Strong Motion Instrumentation Program* [Data set]. International Federation of Digital Seismograph Networks. https://doi.org/10.7914/b34q-bb70

California Institute of Technology (Caltech) (1926). Southern California Seismic Network. International Federation of Digital Seismograph Networks. Other/Seismic Network. https://doi.org/10.7914/SN/CI

Caplan-Auerbach, J., K. Marczewski, and G. Bullock (2023). Beast Quake (Taylor's Version): analysis of seismic signals recorded during two Taylor Swift concerts, PREPRINT (Version 1) available at Research Square. https://doi.org/10.21203/rs.3.rs-3401209/v1

Catbas, F. N., M. Gul, and H. O. Sazak (2010). Dynamic testing and analysis of a football stadium, Proceedings of the IMAC-XXVIII conference, February 1-4, 2010, Jackson, FL.

Chen, J., H. Tan, K. Van Nimmen, and P. Van den Broeck (2019). Data-driven synchronization analysis of a bouncing crowd. *Shock and Vibration*, *2019*. https://doi.org/10.1155/2019/8528763

Denton, P. (2014). One step beyond. *Astronomy and Geophysics*, 55(5), 5-30.

Díaz, J., M. Ruiz, P. S. Sánchez-Pastor, and P. Romero (2017). Urban seismology: On the origin of earth vibrations within a city. *Scientific reports*, *7*(1), 15296. doi:10.1038/s41598-017-15499-y

Ereditato, D., and G. Luongo (1994). Volcanic tremor wave field during quiescent and eruptive activity at Mt. Etna (Sicily), *J. Volcanol. Geotherm. Res.*, 61.

Erlingsson, S., and A. Bodare (1996). Live load induced vibrations in Ullevi Stadium—dynamic dynamic soil analysis. Soil Dynamics and Earthquake Engineering, 15(3), 171-188.

Green, D. N., and D. Bowers (2008). Seismic raves: Tremor observations from an electronic dance music festival. Seismological Research Letters, 79(4), 546-553. https://doi.org/10.1785/gssrl.79.4.546

Jennings, P. C., and H. Kanamori (1983). Effect of distance on local magnitudes found from strong-motion records, *Bull. Seismo. Soc. of Am.*, 73(1), 265-280.

Hough, P. V. (1962). Method and means for recognizing complex patterns. *U.S. Patent No. 3,069,654*. Washington, DC: U.S. Patent and Trademark Office.

Hutton, K., J. Woessner, and E. Hauksson (2010). Earthquake monitoring in southern California for seventy-seven years (1932–2008), *Bulletin of the Seismological Society of America*, 100(2), 423-446.

Kanamori, H., J. I. M. Mori, E. Hauksson, T. H. Heaton, L. K. Hutton, and L. M. Jones (1993). Determination of earthquake energy release and ML using TERRAscope, *Bulletin of the Seismological Society of America*, 83(2), 330-346.

Kanamori, H., P. Maechling, and E. Hauksson (1999). Continuous Monitoring of Ground-Motion Parameters, *Bull. Seism. Soc. Am.*, 89, 1, 311-316.

Kanamori, H., Z. E. Ross, and L. Rivera (2020). Estimation of radiated energy using the KiK-net downhole records-Old method for modern data, *Geophys. J. Int.*, 1029–1042. https://doi.org/10.1093/gji/ggaa040.

Liu, X., F. Xiong, Q. Xie, X. Yang, D. Chen, and S. Wang (2022). Research on the Attenuation Characteristics of High-Frequency Elastic Waves in Rock-Like Material. *Materials*, *15*(19), 6604. https://doi.org/10.3390/ma15196604

Ma, Y., R. W. Clayton, and D. Li (2016). Higher-mode ambient-noise Rayleigh waves in sedimentary basins, *Geophysical Journal International*, *206*(3), 1634-1644. https://doi.org/10.1093/gji/ggw235

Malone, S., K. Hall, L. Simmons, and J. Vidale (2015). How to recognize a "beast quake" and a "dance quake", *Seismological Research Letters*, 86(3), 1006-1008. https://doi.org/10.1785/0220150053

Montalbetti, J. F., and E. R. Kanasewich (1970). Enhancement of Teleseismic Body Phases with a Polarization Filter, *Geophys. J. Royal Astro. Soc.*, 21. https://doi.org/10.1111/j.1365-246X.1970.tb01771.x

Ponti, D. and P. Martin (2021). Development of a chronostratigraphic hydrogeologic framework model, in *Development of a groundwater-simulation model in the Los Angeles Coastal Plain* S. Paulinksi (Editor), Los Angeles County, California, *U.S. Geological Survey Scientific Investigations Report 2021–5088*, 489 p. https://doi.org/10.3133/sir20215088

Richter, C. F. (1935). An instrumental earthquake magnitude scale. Bulletin of the seismological society of America, 25(1), 1-32.

Sahakian, V., J. Bormann, N. Driscoll, A. Harding, G. Kent, and S. Wesnousky (2017). Seismic constraints on the architecture of the Newport-Inglewood/Rose Canyon fault: Implications for the length and magnitude of future earthquake ruptures, J. Geophys. Rev., 122(3), 2085-2105. https://doi.org/10.1002/2016JB013467

Sahlin, S. (1986). Rapport över uppmätning av dynamiska krafter från rythmiskt hoppande människor vid t ex rockgalor. Dept of Struct. Mechanics, Royal Inst. of Tech., Stockholm, Sweden.

Saucedo, G. J., H. G. Greene, M. P. Kennedy, and S. P. Bezore (2003). Geologic map of the Long Beach 30' x 60' quadrangle, California—A digital database: California Geological Survey Preliminary Geologic Maps, scale 1:100,000.

SCEDC. (2013). Southern California Earthquake Center. Caltech. Dataset. https://doi.org/10.7909/C3WD3xH1

Solberg, R. T., and A. R. Jensenius (2019). Group behaviour and interpersonal synchronization to electronic dance music. *Musicae Scientiae*, *23*(1), 111-134. https://doi.org/10.1177/1029864917712345

Styns, F., L. van Noorden, D. Moelants, and M. Leman (2007). Walking on music. *Human movement science*, *26*(5), 769-785. https://doi.org/10.1016/j.humov.2007.07.007

Thompson G., and C. Reyes. (2017). GISMO - a seismic data analysis toolbox for MATLAB [software package], http://geoscience-community-codes.github.io/GISMO/. Accessed October 2023. https://doi.org/10.5281/zenodo.1404723

U.S. Geological Survey. (1931). *United States National Strong-Motion Network* [Data set]. International Federation of Digital Seismograph Networks. https://doi.org/10.7914/SN/NP

U.S. Geological Survey and California Geological Survey. (2023). Quaternary fault and fold database for the United States: U.S. Geological Survey website, accessed September 2023, at https://www.usgs.gov/programs/earthquake-hazards/faults

Wright, T. L. (1991). Structural geology and tectonic evolution of the Los Angeles Basin, California, in *Active margin basins: American Association of Petroleum Geologists Memoir 52* Biddle, K. T. (Editor), 35–79.

Yerkes, R. F., T. H. McCulloh, J. E. Schoellhamer, and J. G. Vedder (1965). Geology of the Los Angeles Basin, California—An introduction, U. S. Geological Survey Professional Paper 420–A, https://doi.org/10.3133/pp420A

Supplemental Material

for

Shake to the beat: Exploring the seismic signals and structural response of concerts and music fans

G. Tepp, I. Stubailo, M. Kohler, R. Guy, and Y. Bozorgnia

Description of supplemental material

This document provides further details about the technical design of SoFi stadium and the speaker experiment, additional figures, and captions for the supplemental data tables. The data tables are provided as individual sheets in the Excel file labeled supplemental_tables.xlsx. We also include SAC data files from the speaker experiment in the zip folder labeled experiment_data.zip.

Supplemental Text

S1: Technical design of SoFi Stadium

The main structural engineering elements of SoFi stadium bowl consist of a steel frame and concrete deck system for lateral and gravity support. The frame is made up of 1100 buckling restrained braces for lateral support. It also has thermal expansion connectors to allow for strain associated with large temperature changes. The decks are composite (concrete) and the seats, stairs, and curbs are pre-cast concrete. The floor level decks consist of corrugated steel overlain by smooth concrete, resulting in a total thickness of several inches. Structural concrete was used to install the slab-on-grade and slab-on-metal deck work.

The stadium roof consists of a canopy supported by 37 reinforced-concrete columns. The roof canopy is made up of a structural steel shell including a compression ring, a cable net system, and over 300 fluorine-based plastic panels covering 1.2 million square feet. Each blade column contains a triple pendulum seismic isolator at the top where the roof meets the column, seismically isolating the roof and shifting the vibration periods to longer periods (e.g., 5 s or longer). The blade columns themselves are expected to have a relatively short period of vibration in the vertical direction (e.g. approximately 0.1 s). While the roof-canopy-column system should not be relevant to this study (as it's separate from the bowl and concert vibration source), it will play an important role in stadium response to future earthquake motions.

Details on structural engineering elements can be found in AISC's Continuing Education series session "Structural Analysis and Design of SoFi Stadium (U3)" presented by R. Sabelli and M.

Waggoner, publicly viewable at https://www.aisc.org/education/continuingeducation/education-archives/structural-analysis-and-design-of-sofi-stadium-u3/.

S2: Detailed description of the speaker experiment

We conducted an experiment to test whether a speaker could feasibly produce the observed low-frequency (1-10 Hz) seismic signals. Two Basalt data loggers with epi-sensors (strong motion accelerometers) were placed 1 m from a speaker system, one in front (CIT-E) and one behind (CIT-T), with the north component parallel to the speaker system (Figure ST1). The front sensor was the same one temporarily deployed during the Swift concerts. Data were recorded at 100 and 200 samples per second. The speaker system was a portable public announcement system (Pyle PWMA1050BT) with 3 built-in speakers (10 inch subwoofer, 4 inch mid range, & 4 inch tweeter), an amplifier with a frequency response down to 35 Hz, and a maximum power output of 800 W (RMS output 400 W, sound pressure level 94 dB re 1 W/m). We performed the experiment in a basement hallway with tile floors. The sensors and speakers were placed on the floor with nothing additional to improve coupling. We initially tested the sensors at a distance of 2 m; however, the signal was too weak to work with, so we moved the sensors closer and successfully made changes to increase the input volume of the music (e.g., switching from an MP3 player to a laptop).

For the music tests, we plugged a laptop into the speaker system and played the song “Love Story” at maximum volume with the Apple Music application (test 1) and at an amplified volume with the Audacity application (test 2), which was loud enough to cause noticeable distortion in the sound. We clearly felt vibrations while standing near the speaker. For both tests, during the last chorus of the song, one person jumped along with the beat in the same way as would be done during a concert. The jumping occurred next to and slightly in front of the speaker (i.e., closer to CIT-E; white X in Figure ST1). For the bass beat test, a bass guitar with active electronics was plugged into the speaker system and played at maximum volume. The bassist finger-picked a low E (lowest note on a typically tuned bass) at 120 beats per minute, first with a metronome and then without. For the last part of the test, the bassist alternated between a low E and the next octave E at a slightly faster pace.

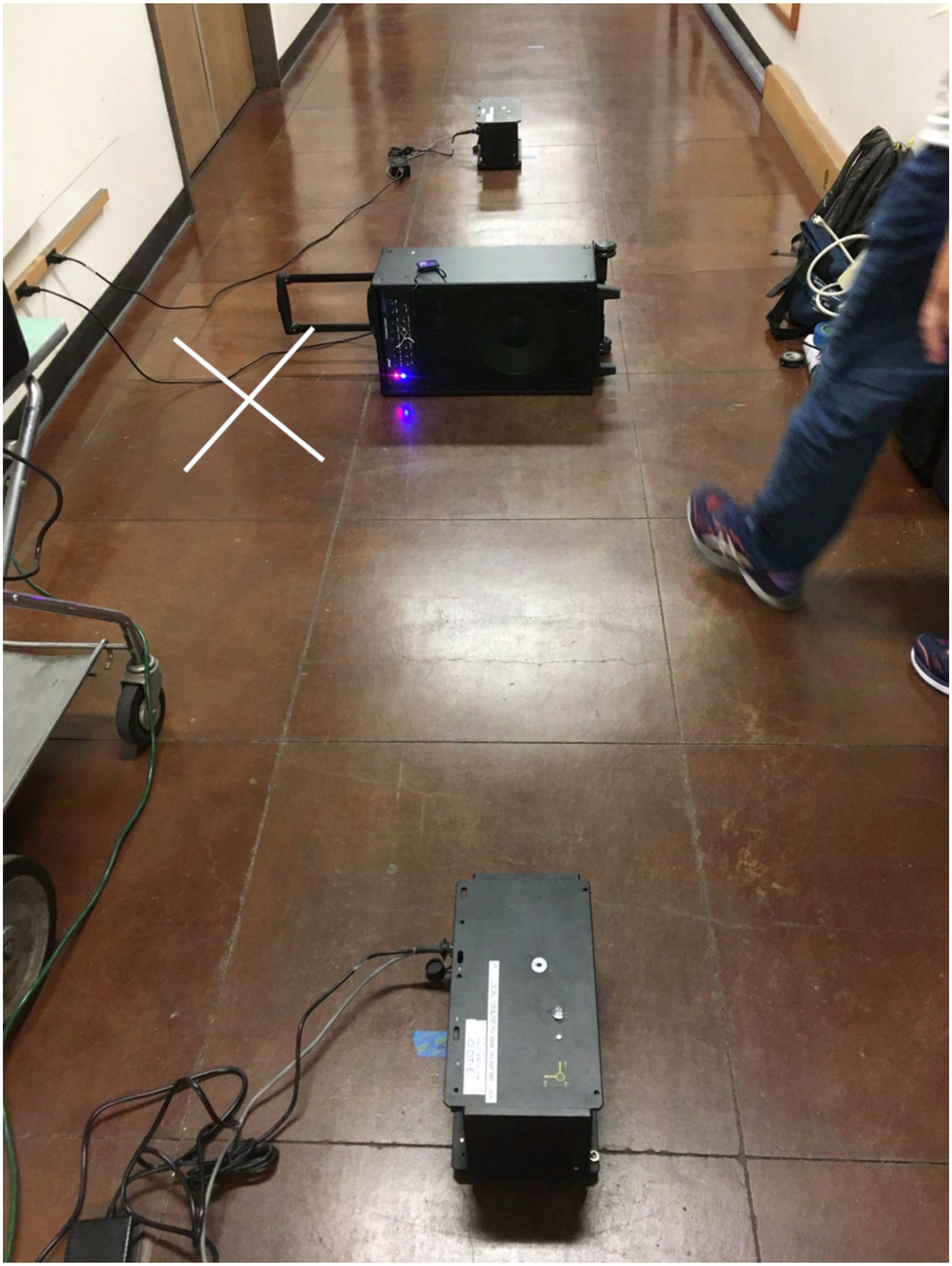

Figure ST1: Experimental setup with two sensors placed on either side of the portable speaker system. Sensors are shown at 2 m distance (center of speaker system to center of blue tape). Yellow arrows visible on the bottom corner of the front sensor indicate north (pointing left) & east directions. The white X approximates the location of the jumping tests.

Supplemental Figures

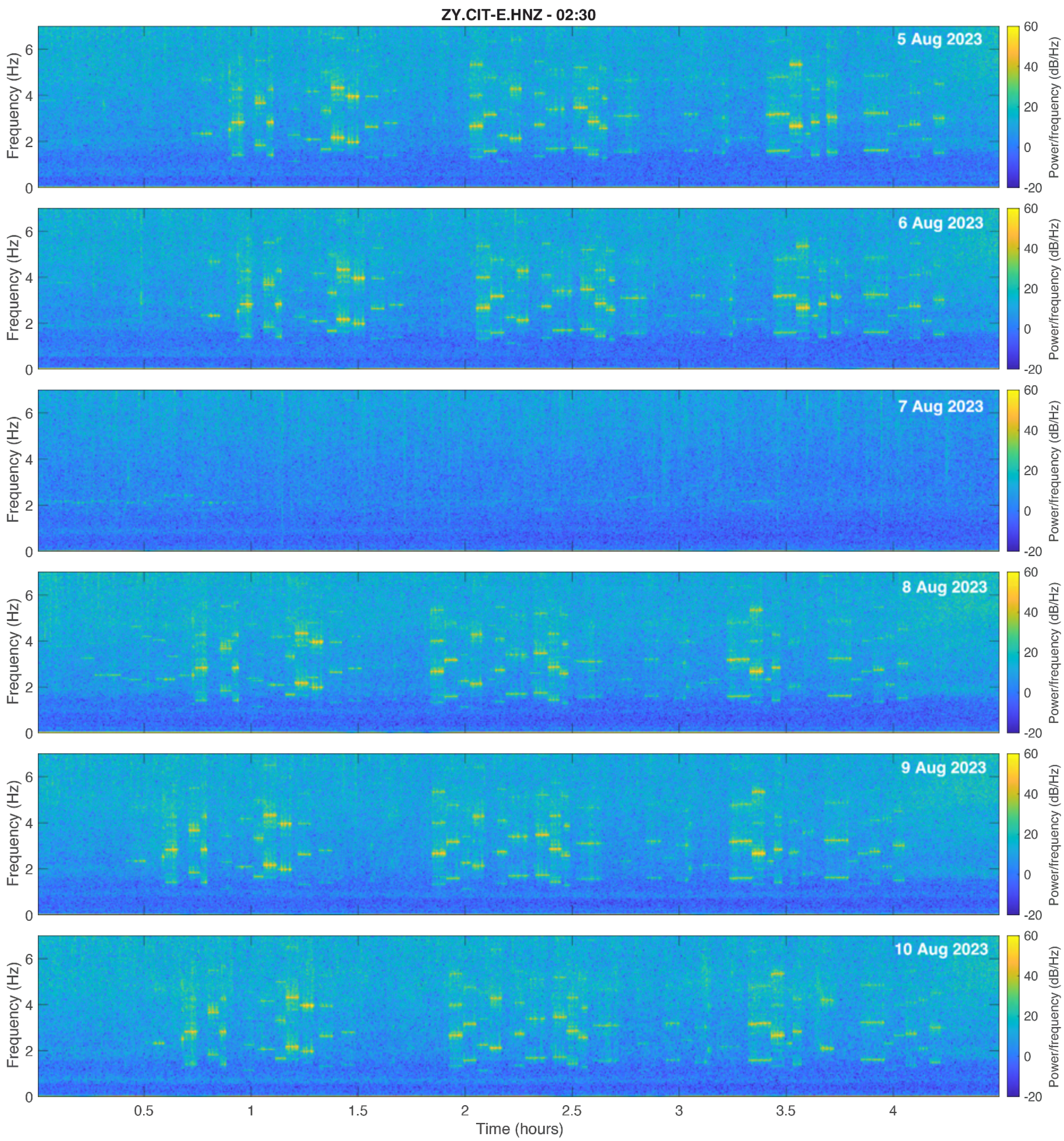

Figure S1: Spectrograms for all six nights recorded by station ZY.CIT-E (02:30-07:00 UTC). Swift concerts occurred every night except 7 August, which was a break in the 6 concert/7 night schedule.

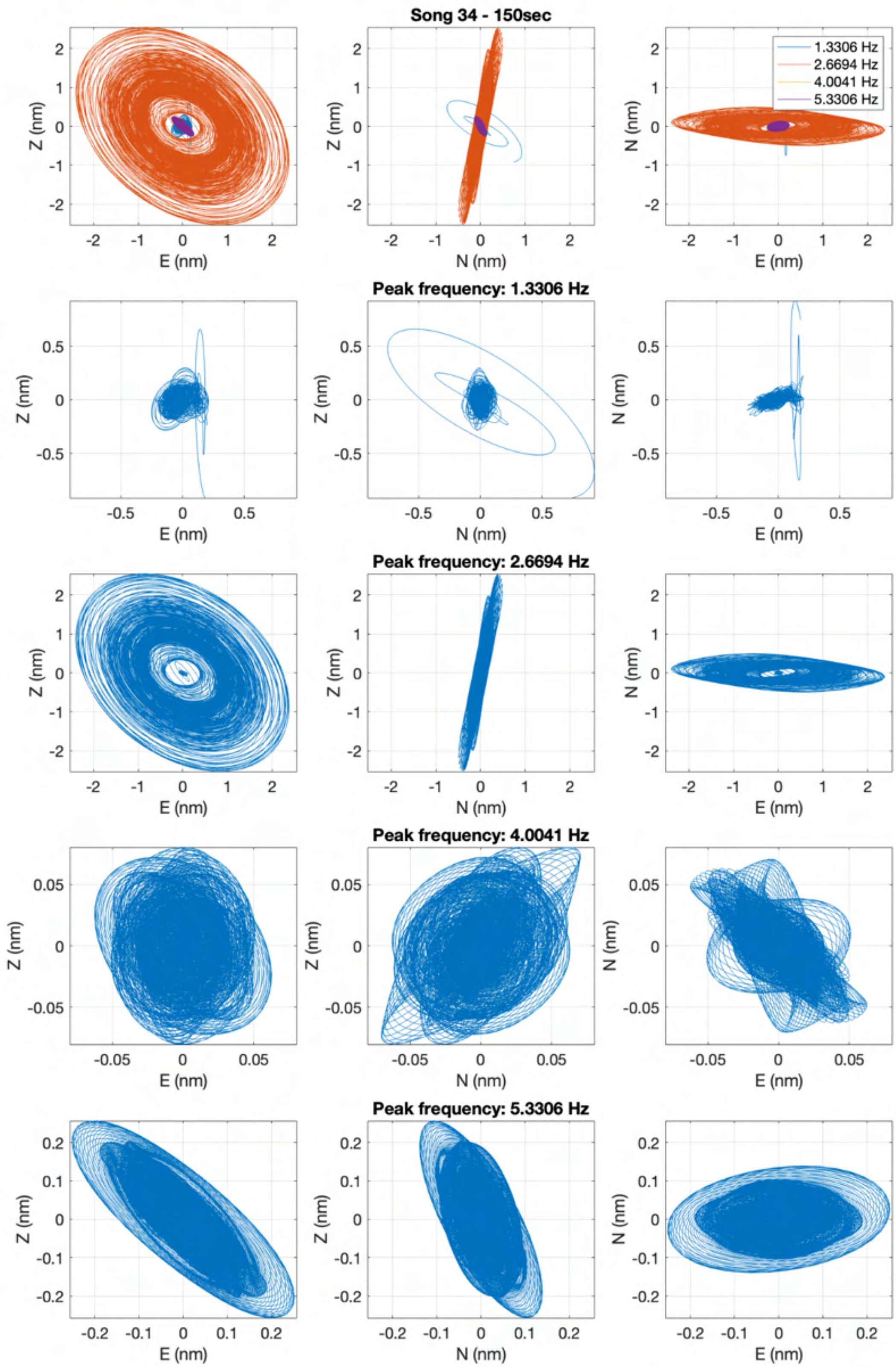

Figure S2: Particle motion on station ZY.CIT-E for song 34 with all harmonics together (top) and each harmonic (frequency peak +/- 0.2 Hz) individually for more detail (rows 2-5).

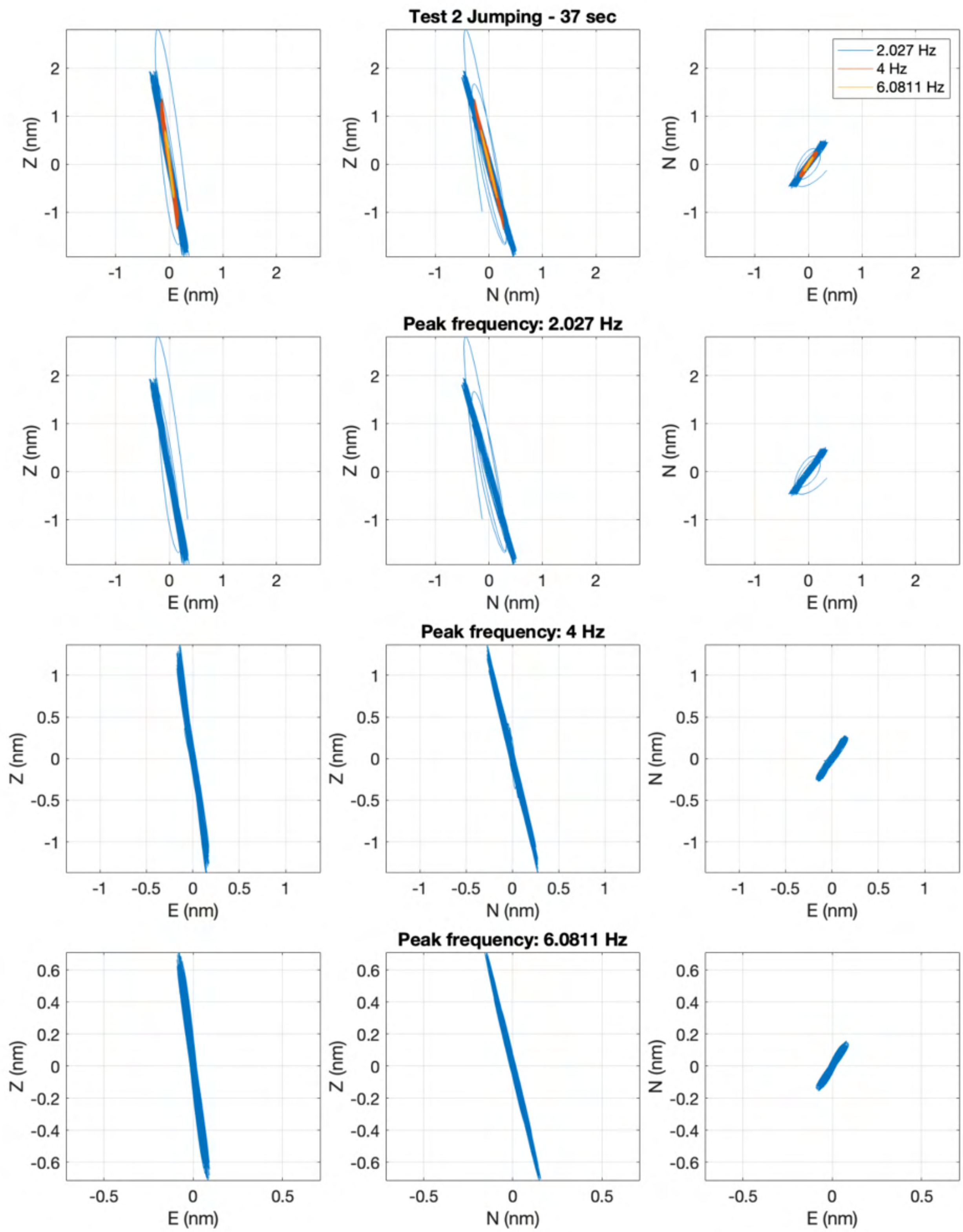

Figure S3: Particle motion of jumping during speaker experiment test 2 from sensor CIT-E (200 Hz data) with all harmonics together (top) and each harmonic (frequency peak +/- 0.5 Hz) individually for more detail (rows 2-4).

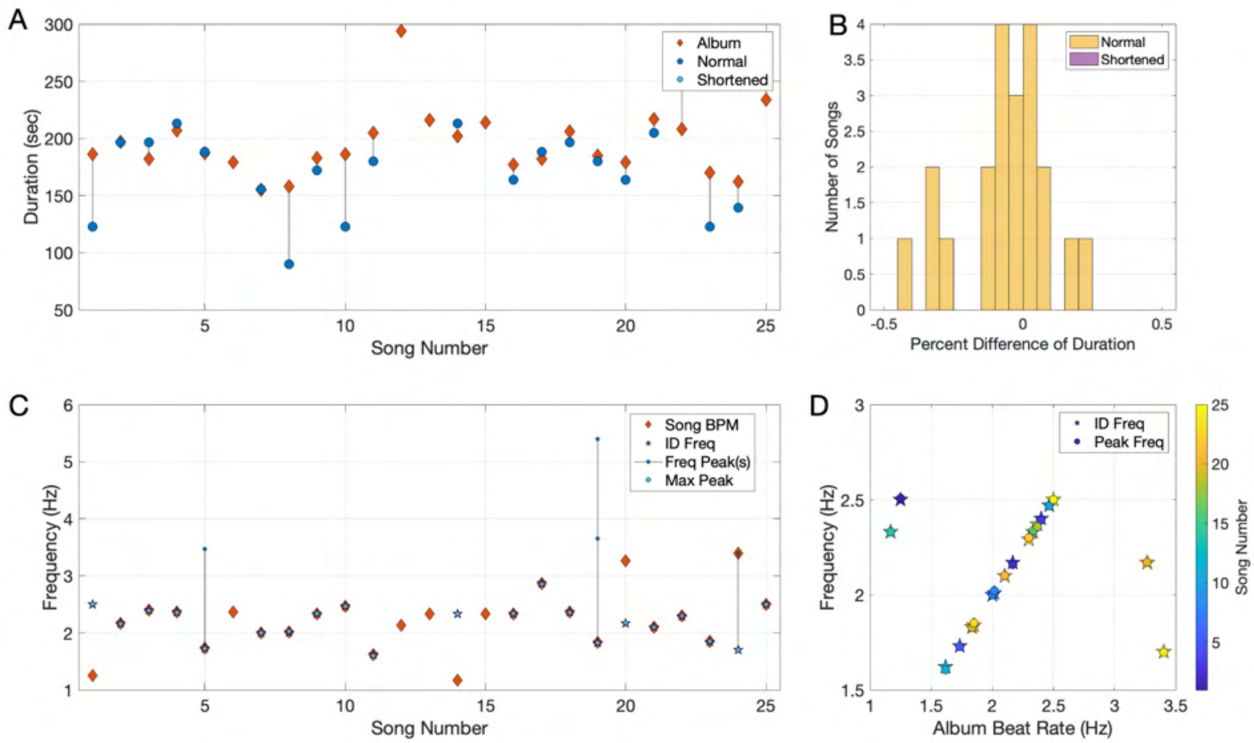

Figure S4: Analysis results for the Wallen concert from station CI.BHP. a) Album and seismic durations of songs in chronological order. “Shortened” refers to songs that were marked as such in the set list, and “normal” refers to the rest. b) Histogram of the percent difference of the seismic duration compared to the album duration. c) Album beats per minute (BPM, red diamonds), the frequency at which the Hough line was identified (magenta star), and frequency peaks from the spectra (blue circles, lighter blue for the strongest peak) for each song in chronological order. d) Comparison of the album beat rates to the identification frequencies (stars) and frequency peaks (circles). “Song number” refers to the index in Table S2.

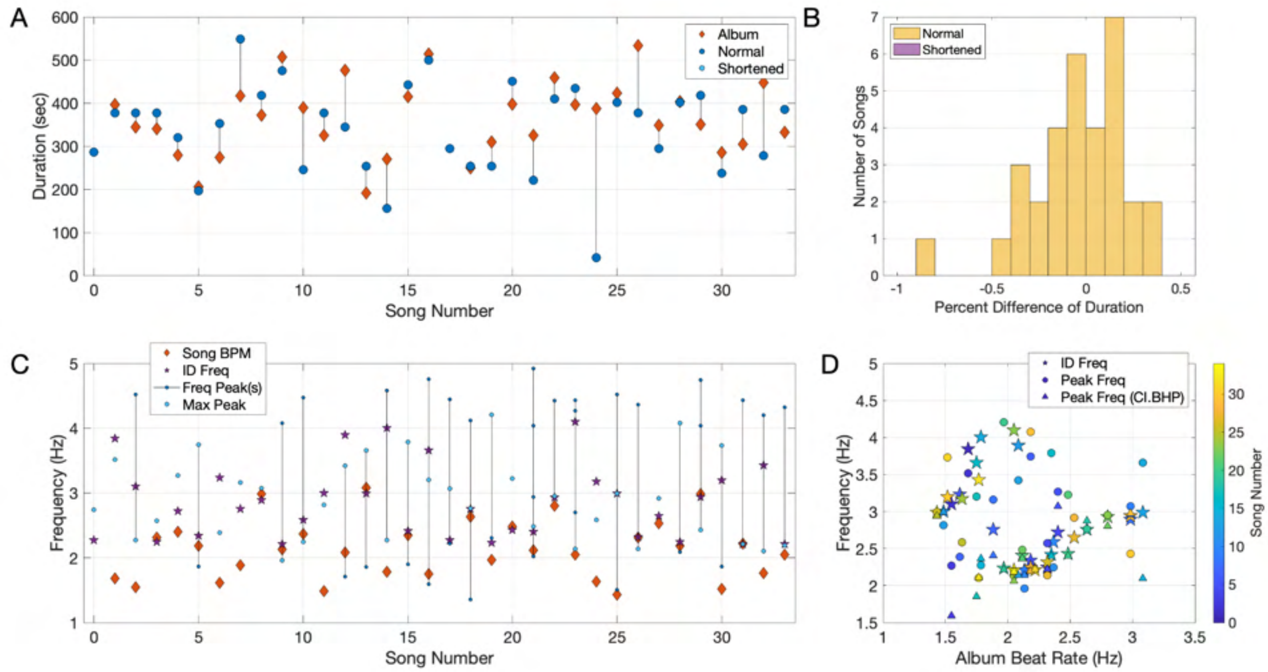

Figure S5: Analysis results for the Metallica concerts from station CE.14683. a) Album and seismic durations of songs in chronological order. “Shortened” refers to songs that were marked as such in the set list, and “normal” refers to the rest. b) Histogram of the percent difference of the seismic duration compared to the album duration. c) Album beats per minute (BPM, red diamonds), the frequency at which the Hough line was identified (magenta star), and frequency peaks from the spectra (blue circles, lighter blue for the strongest peak) for each song in chronological order. d) Comparison of the album beat rates to the identification frequencies (stars) and frequency peaks (circles). “Song number” refers to the index in Table S3.

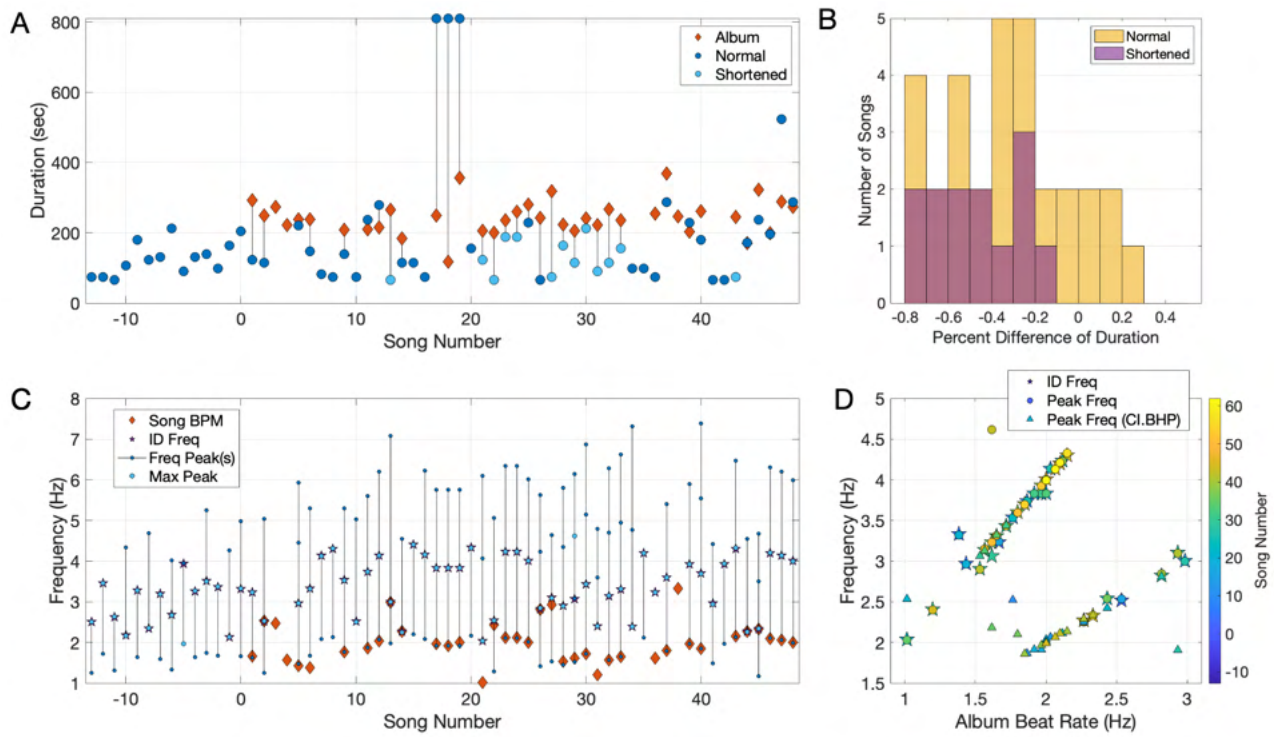

Figure S6: Analysis results for the Beyonce concert from station CE.14683. a) Album and seismic durations of songs in chronological order. “Shortened” refers to songs that were marked as such in the set list, and “normal” refers to the rest. b) Histogram of the percent difference of the seismic duration compared to the album duration. c) Album beats per minute (BPM, red diamonds), the frequency at which the Hough line was identified (magenta star), and frequency peaks from the spectra (blue circles, lighter blue for the strongest peak) for each song in chronological order. d) Comparison of the album beat rates to the identification frequencies (stars) and frequency peaks (circles). “Song number” refers to the index in Table S4 with negative numbers indicating songs from the opening act.

Supplemental Table Captions

Table S1: Analysis details of Taylor Swift concert on 5 August 2023. Columns 3-6 are details of the album recordings. Columns 7-18 are the analysis results from ZY.CIT-E (unless otherwise specified).

Table S2: Analysis details of Morgan Wallen concert on 23 July 2023. Columns 3-6 are details of the album recordings. Columns 7-15 are the analysis results from CI.BHP.

Table S3: Analysis details of Metallica concerts on 26 & 28 August 2023. Columns 3-6 are details of the album recordings. Columns 7-16 are the analysis results from CE.14683 (unless otherwise specified).

Table S4: Analysis details of Beyonce concert on 2 September 2023. Columns 3-6 are details of the album recordings. Columns 7-16 are the analysis results from CE.14683 (unless otherwise specified).